3-D Computation of Plasma Thruster Plumes

Passaro A.[*]
Aerospace Division – CPR, Ospedaletto, Pisa, 56121, Italy

Vicini A.[†] and Biagioni L.[‡]
Alta S.p.A. – via Gherardesca 5 – Pisa, 56121, Italy

Electric propulsion represents one of the most promising technologies for application in future space missions. The knowledge of the plasma plume evolution in the thruster surrounding space is still of fundamental importance, at system design level, for new generation satellites, in order to integrate the propulsive subsystem with the other vehicle subsystems. Furthermore, the necessity to simulate realistic configurations leads to the need of powerful and flexible 3-D tools. Alta S.p.A. and Consorzio Pisa Ricerche developed a three-dimensional particle-in-cell code capable to simulate conditions found both in space and in ground vacuum facilities, for realistic satellite configurations for Hall Effect Thrusters and Gridded Ion Engines. The present article will present a brief description of the PICPluS 3D code, including the various physical models that can be used and the code validation. Numerical results related to the ESA's SMART-1 satellite, launched on 27 September 2003, will then be compared with flight data. Finally, an analysis of the influence of the simulation paramaters on the results will follow.

Nomenclature

e	=	electron charge
k	=	Boltzmann constant
m_T	=	propellant mass-flow rate
n	=	number density
T	=	temperature
Te	=	electron temperature
α	=	exponent for the adiabatic electron temperature model
γ	=	ratio of gas specific heats
φ	=	electrostatic potential

I.   Introduction

Electric propulsion represents one of the most promising technologies for application in future space missions, in particular for the relatively high thrust capability of electric thrusters, coupled with a specific impulse which is up to one order of magnitude higher than latest generation chemical systems. In the recent years the first western missions have seen successful use of Gridded Ion Engines (Deep Space 1, Artemis) and Hall Effect Thrusters (SMART-1): nonetheless, at the present state of knowledge, a great effort on ground characterization within proper vacuum chamber based facilities is still needed.

Alta and Consorzio Pisa Ricerche (CPR) in Pisa, Italy, have dedicated the last few years to develop a series of numerical engineering tools to be used along with their wide array of vacuum facilities for the design, test, and qualification of electric thrusters. In particular, three numerical codes were developed: one charge neutral 3D DSMC code able to predict operational parameters of realistic complex vacuum test systems, including the peculiar pumping system arrangement used[1]; one axysimmetric and one three-dimensional *hybrid* PIC DSMC[2,3,4] codes (PICPluS-2 and PICPluS-3D), able to simulate plume expansions of HET and GIE considering the satellite shape or the ground facility environment and geometry in simplified form, and with the possibility of using several different

---

physical models. All of the codes were validated against literature data and results of experiments carried out within Alta facilities.

The present paper will focus on the results of the PICPluS 3D code applied to the SMART-1 mission: the following sections will provide a brief overview of the code features and validation and will be followed by a more detailed analysis of the code predictions compared with the in-flight data, focussing on the effect of the chosen physical models on the numerical results.

II. Code description
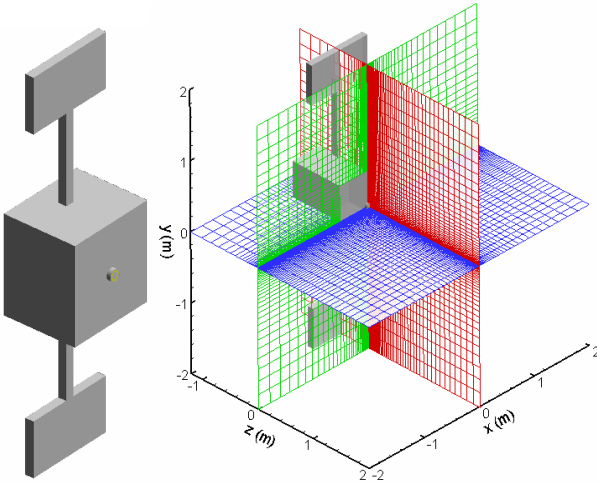
Figure 1.   PICPluS 3D geometry model and grid for the SMART-1 satellite in flight configuration with unfolded solar panels (truncated at 2 m from the thruster exit).

PICPluS 3D is a three-dimensional hybrid PIC code, directly obtained by the axy-symmetric version developed earlier at Alta[5,6]. The code uses a structured grid, based on a non-uniform Cartesian mesh, with the possibility of inclusion of different thruster units and solid bodies that can be constituted by boxes or by *zero-thickness* lines and surfaces (plain or cylindrical). It requires as input data ions and neutral distribution at the exit of the acceleration channel as well as magnetic field components (assumed constant during the simulation) on the whole simulation grid. Experimental data or results of channel simulation can be used via an internal interpolation routine that allows to adapt any kind of data on the chosen computational grid. Furthermore, a procedure able to extend results from 2D simulation to fully 3D configurations was developed. The code is optimised in order to run on a single PC workstation and can manage up to 5 million particles on grids with typical length of some meters, in vacuum conditions, in less than 24 hours of computation.

Several physical models, that will be illustrated in the following sub-sections, can be used in order to describe plasma properties, collisions, and interaction with solid walls; a set of virtual plasma probes (Faraday's cups and RPA's) can be included everywhere in the simulation domain.

A. Plasma Dynamics

The plasma potential is obtained by the hypothesis of quasi-neutrality, and thus equaling the electron density to the ion density. Assuming that electrons are collision-less and un-magnetized, and that their pressure obeys the ideal gas law, the Boltzmann relation is obtained for the plasma potential:

$$\varphi - \varphi^* = \frac{kT}{e}\ln\left(\frac{n}{n^*}\right) \tag{1}$$

where superscript * indicates a reference state. The electric field is obtained through spatial differentiation of the plasma potential. Electron temperature in eq.(1) may be held constant. However, as experimental evidence indicates that electron temperature is not constant, an adiabatic model[7] can be used to relate its changes to changes in electron density:

$$T = T_{ref}\left(\frac{n}{n_{ref}}\right)^{\alpha-1} \tag{2}$$

where α is a number than can be set between $\gamma = c_p/c_V = 5/3$ (monoatomic gas) and 1 (isothermal case); in this case the electron temperature field is updated at each time step. A static magnetic field can also be included in the simulation.

B. Ions and Neutrals

Several particle species can be independently simulated (neutral atoms, single and doubly charged ions). Xenon propellant is currently used, but other propellants can be added. Background distributions of neutral propellant are included in the simulation. Neutral atoms, possibly exiting from the thruster due to the effective ionization rate, are also simulated (either through a MCC or DSMC approach[2,3]).

C. Collision Dynamics

Neutral-neutral and ion-neutral (elastic and Charge Exchange) collisions can be included in the PIC cycle independently. In the case of atom-atom collisions, the Variable Hard Sphere (VHS) model is employed. For atom-ion collisions, the VHS model or the induced dipole model of Nanbu[6,8] can be used; in the latter case, no collision cross sections need to be modeled.

D. Computational Grid

The computational grid is cartesian, non uniform in every direction in order to adapt to the local plasma density in a simple and straightforward way. This allows to model fairly complex geometries, while providing good computational efficiency for particles tracking operations (Fig.1).

E. Boundary conditions

The boundaries of the simulation domain can be considered as outflow or as solid walls; in the latter case their temperature and potential are assigned, and ion impacts may range between perfect reflection and full random diffusion, with partial thermal accommodation calculated using Cercignani-Lampis-Lord model[2]. In the same manner internal solid boundaries can be modeled.

Data regarding the plasma characteristics at the exit of the thruster (potential, number densities, velocities) can be customized so as to represent the desired distributions starting from experimental or numerical data on any grid, using the code internal advanced interpolation features (Fig. 2).
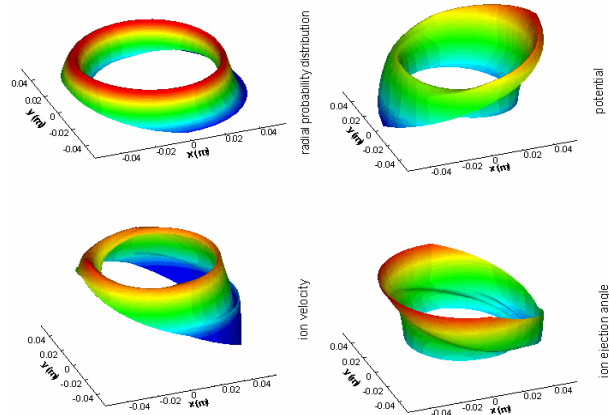
Figure 2. 3D injection probability distribution obtained from 2D simulation results for non axisymmetric inlet conditions.

III. Code verification and validation

The PICPluS 3D simulation code has been assessed firstly comparing results obtained with the ones produced by PICPluS 2 and then comparing directly the code prediction with literature experimental data. This procedure allowed to identify the range of applicability of the two-dimensional axy-symmetric code and, at the same time, the differences obtained considering axy-symmetric or Cartesian equations and geometries. Due to the wide range of literature data, one of the chosen test cases for verification and validation was the study of a SPT-100 plume in standard configuration with comparison of plasma properties close to the thruster exit and downstream the plume. The second test case was the SNECMA PPS®1350, which is also present on the SMART-1 satellite[9], in vacuum chamber conditions. In particular, the references for the test case simulations are indicated in the following Table 1 while part of the results is presented in the successive figures.

Thruster Model	Vd [V]	Id [A]	Anode Mass Flow-rate [mg/s]	Background Pressure [mbar]	Ref.
SPT-100	300	4.5	4.99	$2.9 \cdot 10^{-6}$	10
SPT-100	300	4.5	5.12	$4 \cdot 10^{-5}$	11
SPT-100	300	4.5	5.084	$5.32 \cdot 10^{-5}$	12
PPS-1350	350	3.47	4.21	$1 \cdot 10^{-4}$	---

Table 1. Test case matrix for the code validation.

F. SPT-100

Data measured by Manzella[10], Kim[11], and King[12] were satisfactorily reproduced using a single set of injection conditions by both PICPluS 2 and PICPluS 3D codes as shown on Fig. 2. The difference on beam current density between 3D data and experiment at high angles is due to the long computation times needed for a three-dimensional simulation to *fill* the whole domain, in particular in the back-flow region. In fact, one of the key differences between axi-symmetric and 3D simulations seems to be due to the fact that, in order to limit the computation time and the number of simulated particles, a coarser grid is necessary for 3D simulations, forcing therefore some (limited) grid effects on the results. From a physical point of view it appears that, for an axi-symmetric simulation, slightly higher levels of electron temperature are obtained in the near field w.r.t to the 3D results, starting from exactly the same initial conditions.

G. PPS®1350

Data measured during a ground test of the PPS®1350 were made available by SNECMA for a Faraday's cup rake situated at 0.65 m from the thruster exit and run with a probe bias of some Volts. Of course, as already mentioned by Van Gilder and Boyd[13], the most important parameter determining plume behavior appears to be the inlet distributions used for ion injection: starting from the SPT-100 typical inlet distributions it was possible to identify the injection parameters able to best reproduce the experimental data, obviously including a proper probe bias, that were then used for 2D and 3D simulations. The two codes results agree fairly well (Fig. 3) for what concerns the simulation in ground conditions while a certain discrepancy (about 5 deg) can be individuated in simulation for
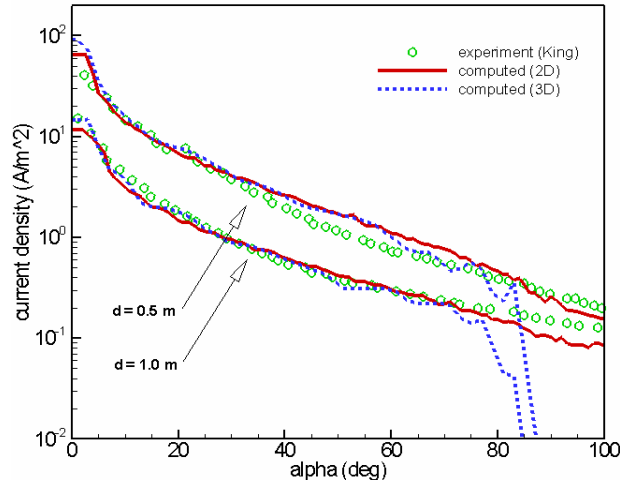
Figure 3. Comparison between 2D, 3D, and experimental data by King for the SPT-100 thruster in vacuum chamber conditions.
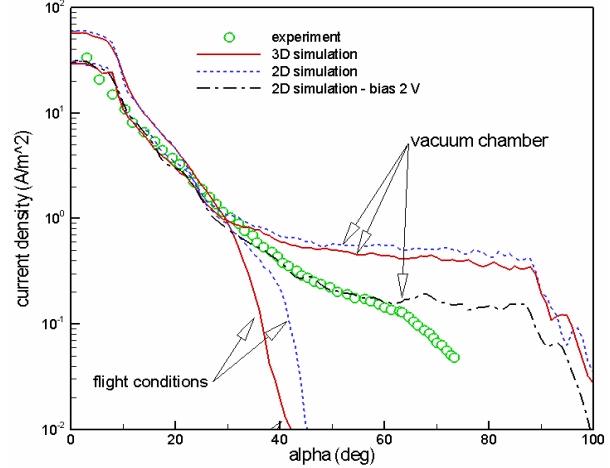
Figure 4. Comparison between 2D, 3D, and experimental data for the PPS-1350 thruster in vacuum chamber conditions.

flight conditions at angles greater than 30 deg, due to the heavy effect that, in this case, is played by the electron temperature model.

IV. Comparison with flight data: SMART-1

SMART-1 is the first ESA Small Mission for Advanced Research & Technology, conceived to demonstrate the operation and the effectiveness of the Solar Electric Propulsion for deep space cruising in preparation of future ESA Cornerstone missions such as the Bepi-Colombo mission to Mercury. Successfully launched on September 27th 2003, the SMART-1 satellite aims at reaching the Moon and to orbit it for a nominal period of 6 months. The selected strategy for the orbit raising consists of extensive HET use for progressively expansion of the spacecraft orbit, spiralling out from the initial GTO until the spacecraft is caught by the Moon's gravitational field. The monitoring of the operation/environment of the EP system, during the orbit transfer from GTO to the final lunar
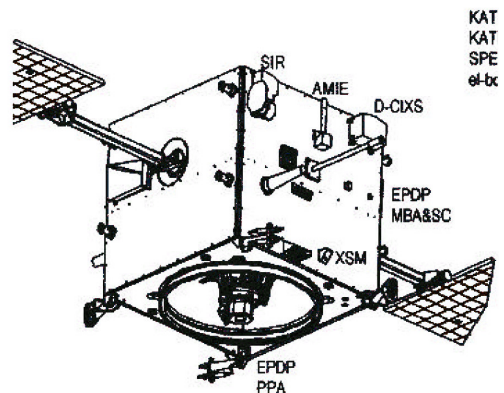
Figure 5. The SMART-1 satellite

orbit, is retained a key issue related to the SMART-1 technology objectives: for this task a specific instrument, the Electric Propulsion Diagnostic Package (EPDP), has been developed by LABEN Proel Tecnologie Division (LABEN/Proel)[14]. The EPDP operates on SMART-1 in conjunction with another instrument, SPEDE (Spacecraft Potential Electron and Dust Experiment), to achieve a comprehensive evaluation of performance and effects of the HET EP based on the PPS®1350 thruster developed by SNECMA. While the EPDP provides information on the plasma environment near the thruster, SPEDE characterizes the plasma on the spacecraft sides. The EPDP on SMART-1 is primarily intended to be operated, together with the thruster, during the spiralling escape maneuvers around the Earth, and the capture of the Moon orbit. The EPDP can be operated according to a suitable set of commands and collects information on the following areas:

Figure 6.   The LABEN/Proel EPDP unit

  – energy/current distribution of plasma ions close to the plasma beam
  – plasma electronic parameters (e.g. plasma density, potential and electron temperature)
  – material erosion/deposition at the Quartz Crystal Microbalance location
  – Solar Cell performance (V-I measurement in open, load, short condition).

A. Simulation results: comparison with flight data and analysis

   A set of numerical simulations was executed with the PICPluS 3D on the grid shown in Fig. 1 considering for all of the cases the standard injection conditions shown in Table 2. The results were compared with EPDP data considering a virtual RPA probe placed in the exact EPDP location, and considering plasma features at the same place.

Mass flow rate	$4.21 \cdot 10^{-6}$ kg/s
Discharge voltage	350 V
Discharge current	3.47 A
Thrust	72.1 mN
Background pressure	$1 \cdot 10^{-9}$ Pa
Ionization efficiency	90%
Percentage of Xe^{++}	25%
Electron temperature model	Adiabatic ($\alpha = 4/3$) or Constant
Potential field	Quasi-neutral
Potential on solid walls	0 V
Neutral atoms plume	Pre-computed

Table 2. Simulation parameters.

   Looking the RPA flight data (Fig. 7) two peculiar features are evident: first of all the energy distribution presents a plateau after the primary peak with a long tail reaching energies up to 100 eV, compatible with the presence of a secondary peak situated about 20 V after the first. Secondarily, the primary peak seems to have a somewhat higher-than-expected energy while a peculiar absence of low energy impinging ions is noted.

   The first set of simulations, conducted with the adiabatic model for electron temperature (with typical value of about 8 eV at the channel exit) produced a remarkably similar pattern for the RPA measurement although *shifted* by almost exactly 18 V towards lower energies. At the same time, it was noted from flight data that an almost constant gap of 18 V was present between RPA first peak position and the satellite floating potential: a possible explanation to this feature could be thought as
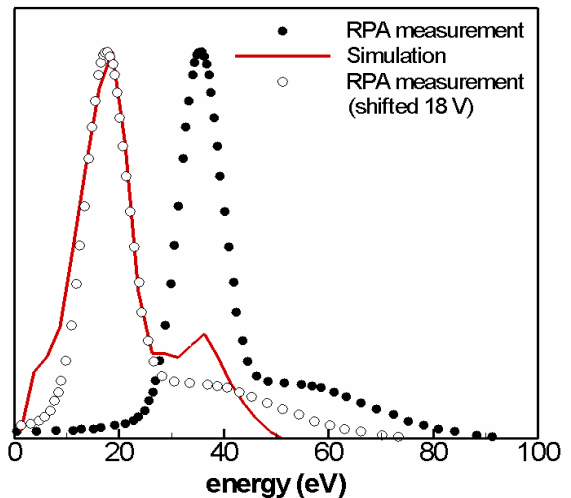
Figure 7.   Comparison between numerical results and flight data for the RPA measurements.

American Institute of Aeronautics and Astronautics

deriving from some kind of insulation loss or grounding between the probe and the satellite body.

It was therefore decided to extend the investigation towards two different directions: assessment of the effect of the electron temperature model and actual value on the results, and assessment of the effect of the presence of Xe^{++} ions in the flow leaving the thruster. A total of 8 numerical test cases was run with the results synthesized in the following Table 3 for the six runs concerned with the electron temperature model.

Case	T_e model	T_e Ref [eV]	Collisions model	RPA Peak 1 [V]	RPA Peak 2 [V]	Peak distance [V]	FWHM [V]	EPDP rel. pot. [V]	EPDP Te [eV]	EPDP n_i x 10^{13} [m^{-3}]
1	Adiabatic	8	Nanbu	18.8	36.1	17.3	12.9	-2.0	0.50	3.7 - 7
1b	Adiabatic	8	VHS	19.0	38.5	19.5	12.8	-2.2	0.56	3.6 – 7.2
2	Adiabatic	12	Nanbu	27.1	49.2	22.1	13.5	-5.1	1.00	7 – 9
3	Adiabatic	16	Nanbu	33.5	68.4	34.9	19.1	-5.5	1.10	5.4 – 6.8
4	Constant	3	Nanbu	26.3	43.8	17.5	11.6	-18.8	3.00	4.1
5	Constant	8	Nanbu	68.0	128.0	60.0	39.0	-50.0	8.00	3.2
EPDP flight data				35.6	55	19.4	13	+4	0.62-0.72	6.8 – 8.7

Table 3. Simulation results compared with EPDP data.

For what concerns the electron temperature model effect it appears that, using the adiabatic model, realistic values for T_e and ion number density are obtained in the EPDP position compared to the flight data. It can be noted that the instrument seems to lay on the edge of the plasma plume and therefore be subject to relatively high variations of ion number density (e.g. for case 1 between $3.7 \cdot 10^{13}$ and $7 \cdot 10^{13}$ m^{-3}); the possibility of EPDP location within the plasma sheath is consistent with the fact that the EPDP individuated a slightly non-neutral plasma. The plasma potential relative to the satellite surface is always predicted as slightly negative (between -2 V and -5 V) while the corresponding measurements present an almost constant value of +4 V. An increase in the T_e reference value corresponds to a shift of the RPA peaks towards higher values with an overall *broadening* of the primary peak
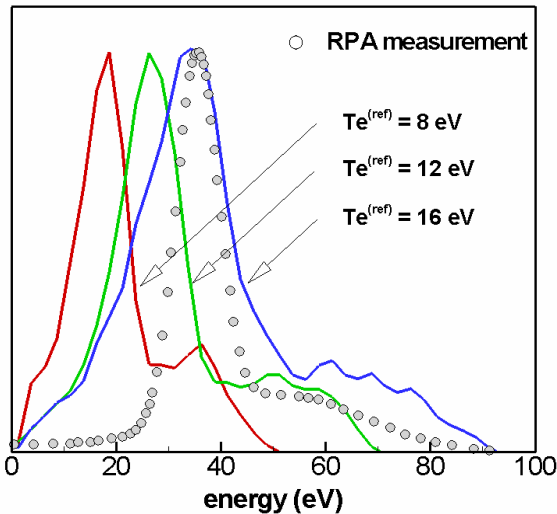
Figure 8. Effect of adiabatic model for electron temperature.
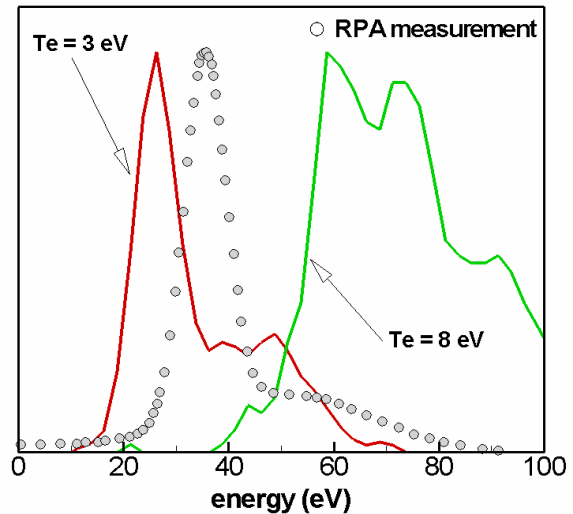
Figure 9. Effect of constant electron temperature.

and an increasing separation of the two peaks; a significant part of low energy events is recorded in any case.

The use of a constant value for T_e produces RPA distributions which are closer to the flight data for what concerns the low energy values but usually tend to present a too high secondary peak w.r.t the first one. Electron temperature value and relative potential are extremely different from the recorded ones, while ion number density is less than expected and close to the low limits for the adiabatic cases. An increase in the temperature value produces a significant shift of the peaks towards higher energies (as also noted by Boyd in Ref. 15).
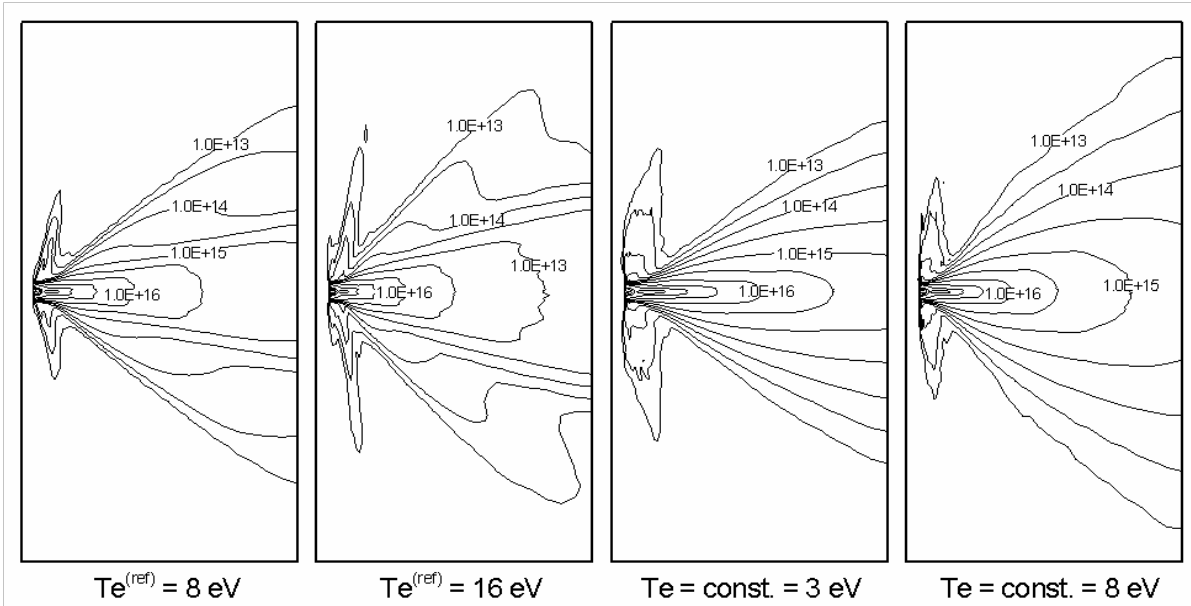
Figure 10.   Comparison between computed ion number densities for test cases 1, 3, 4, and 5.

Considering the effects of the chosen electron temperature model on the whole plume shape (Fig. 10), one can observe that, in general, an increase of the reference T_e produces a wider plume with a stronger expansion in the axial direction. The choice of constant electron temperature tends to spread the CEX cloud that forms close to the satellite wall due to the migration of the CEX ions that are mainly generated at the exit of the acceleration channel.
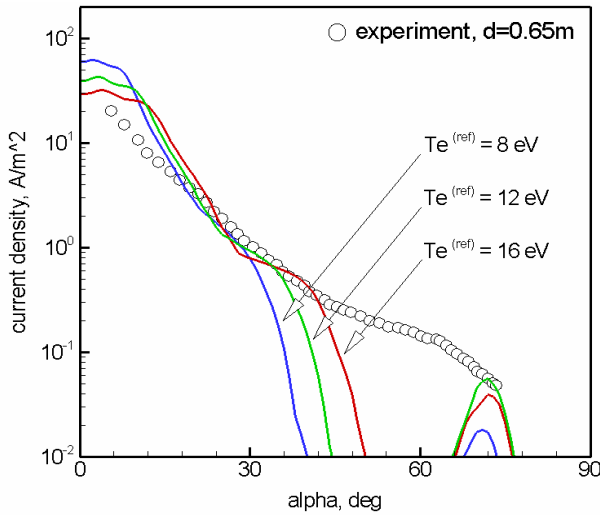
Figure 11.   Effect of adiabatic T_e model on beam current density: comparison between numerical flight results and ground data.
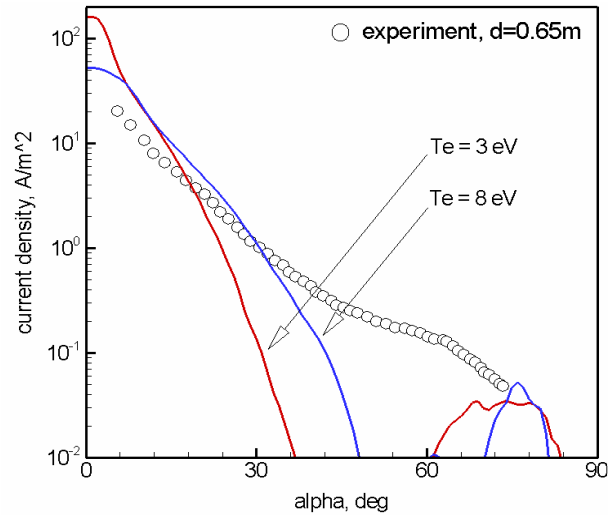
Figure 12.   Effect of constant T_e on beam current density: comparison between numerical flight results and ground data.

The effect of the electron temperature model on the beam current density is shown in Fig. 11 and Fig. 12. For both choices (adiabatic model or constant T_e) it can be seen how the increase of the temperature reference value corresponds to a widening of the plume half-angle (see also Fig.10), with a corresponding lowering of the peak value on the axis, due to the increased CEX formation ratio at the exit of the acceleration channel. Besides, the constant electron temperature provides a different shape of the current density curves, with a much less pronounced inflection point at low angles.

Summarizing these considerations it seems that the best way to reproduce the measured data is using the adiabatic T_e model with a reference electron temperature between 8 and 12 eV, *and* considering a certain shift to be imposed on the experimental data maybe due to some grounding problem.

The effect of the double charged ions presence is evidenced in Fig. 13 where it can be noted that, if no Xe^{++} are simulated, the RPA profile is completely different from the flight one, while a percentage of at least 20% of Xe^{++} seems needed in order to reproduce the second peak and plateau features. This is in accordance with basic theoretical calculations on thruster performance, that see as necessary a similar percentage of double charged ions in order to have the prescribed discharge current, voltage and thrust.

Finally, it has to be noted that, as it was likely to be expected, the simulations for flight conditions predict a higher thrust level (up to +10%) than the one measured on ground and this feature has been observed consistently within the more than 2000 hours of firing of the thruster for the orbit raising.
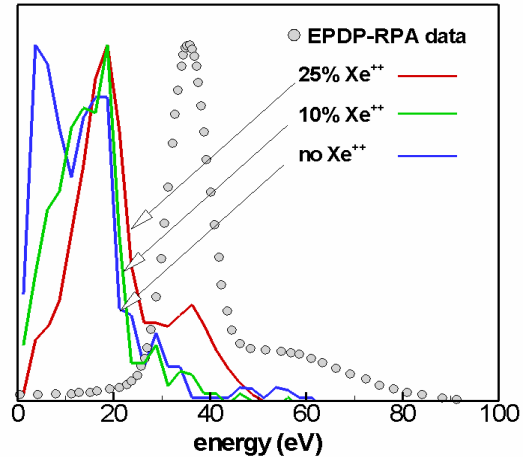
Figure 13. Comparison between numerical results and flight data for the RPA measurements.

V.   Conclusions

Plasma thrusters represent an extremely interesting technology for future space applications, but still need, at the present state knowledge, a great effort on ground characterization within proper vacuum chamber based facilities and through detailed numerical simulations. In particular, the need of simulation within realistic conditions, both for geometry and physical models, brings to the necessity of flexible 3D tools, capable to provide reasonable results in short times. During the last few years, CPR and Alta SpA dedicated consistent efforts in order to individuate and develop a series of simulation instruments that can be used for design or diagnostic purposes. This paper focused on the PICPluS 3D code, showing the results obtained for the SMART-1 satellite and comparing them with the in-flight data provided by the satellite instruments. An analysis of the influence of electron temperature model and of the presence of doubly charged ions was therefore conducted leading to results that are in satisfactory agreement with the flight data.

Acknowledgments

References

[1.] Biagioni, L., Passaro, A., Andrenucci, M., "Particle Simulation of Tailored Vacuum Pumping Configurations for Electric Propulsion Testing", presented at the 4th International Symposium on Environmental Testing for Space Programmes Liege, June 2001.

[2.] Bird, G.A., *Molecular Gas Dynamics and the Direct Simulation of Gas Flows*, Oxford Science Publications, Oxford, 1994.

[3.] Birdsall, C.K., Langdon, A.B., *Plasma Physics Via Computer Simulation*, McGraw-Hill, New York, 1985.

[4.] Hockney, R.W., Eastwood, J.W., *Computer Simulation Using Particles*, McGraw-Hill, New York, 1981.

[5.] Andrenucci, M., Biagioni, L., Passaro, A., "PIC/DSMC Models for Hall Effect Thruster Plumes: Present Status and Ways Forward", AIAA Paper 2002-4254, July 2002.

[6.] Biagioni, L., Passaro, A., Vicini, A., "Plasma Thruster Plume Simulation: Effect of the Plasma Quasi Neutrality Hypothesis"*,* 34th AIAA Plasmadynamics and Lasers Conference, Orlando FL , 23-26 June 2003.

[7.] Celik, M., Santi, M., Cheng, S., Martinez-Sanchez, M., Peraire, J., "Hybrid-PIC Simulation of a Hall Thruster Plume on an Unstructured Grid with DSMC Collisions", presented at the 28th IEPC, Toulouse, March 2003.

[8.] Nanbu, K., (2000), "Probability Theory of Electron-Molecule, Ion-Molecule, Molecule-Molecule, and Coulomb Collisions for Particle Modeling of Materials Processing Plasmas and Gases", *IEEE Transactions on Plasma Science*, Vol.28, No.3.

[9.] Koppel, C. R., Estublier, D., "SMART-1 Primary Electric Propulsion Sub-System – The Flight Model", presented at the 28th IEPC, Toulouse, March 2003.

[10.] Manzella, D.H., Sankovic, J.M., "Hall Thruster Ion Beam Characterization", AIAA Paper 95-2927, July 1995.

[11.] Kim, S. W., Foster, J. E., Gallimore, A. D., "Very Near Field Plume Study of a 1.35 kW SPT-100", AIAA Paper 96-2972, July 1996.

American Institute of Aeronautics and Astronautics

12. King, L.B., "Transport Property and Mass Spectral Measurements in the Plasma Exhaust Plume of a Hall Effect Space Propulsion System", Ph.D. Dissertation, Dept. Of Aerospace engineering, Univ. Of Michigan, Ann Arbor, MI, May 1998.

13. Van Gilder, D.B., Boyd, I.D., "Particle Simulations of the SPT-100 Plume", AIAA Paper 98-3797, 1998.

14. Matticari, G., Noci, G., Estublier, D., Gonzales del Amo, J., Marini, A., Tajmar, M., "The Smart-1 Electric Propulsion Diagnostic Package", *Proceedings of the 3rd Spacecraft Propulsion Conference*, 2000.

15. Boyd, I. D., "Hall Thruster Far Field Plume Modeling and Comparison with EXPRESS Flight Data", AIAA Paper 2002-0487, 2002.